Progress report from the XMM Medium Deep Survey

M. Tajer[1,2], L. Chiappetti[3], G. Trinchieri[1], L. Maraschi[1], D. Maccagni[3], M. Pierre[4] and J. Surdej[5]

[1] *INAF Osservatorio Astromomico di brera, via Brera 28, 20121 Milano, Italy*
e-mail: tajer@brera.mi.astro.it
[2] *Università di Milano – Bicocca, Dipartimento di Fisica, P.za della Scienza 3, 20126 Milano, Italy*
[3] *INAF/CNR IASF, Sezione di Milano, via Bassini 15, 20133 Milano, Italy*
[4] *CEA/DMS/DAPNIA, Service d'Astrophysique, Saclay, France*
[5] *Institut d'Astrophysique et de Géophysique, Université de Liège, Belgium*

ABSTRACT
We present here the XMM Medium Deep Survey (XMDS), a project aiming to obtain a multiwavelength coverage of a contiguous area of about 2 deg^2 of sky, in order to determine large scale structures and AGN correlation function. We focus our analysis on X-ray sources detected above the 4 σ significance level in at least one of the energy bands considered and with optical information. We discuss their X-ray and optical properties and confirm that hardness ratio together with X-ray - to - optical ratio allows us to discriminate between stars and extragalactic population.

1. INTRODUCTION

The XMM Medium Deep Survey (XMDS) is a joint program that involves three XMM hardware institutes (IASF Milan, Italy, CEA Saclay, France, Université de Liège, Belgium). The XMDS aims at obtaining a deep multiwavelength coverage of a contiguous area of about 2 deg^2. Unlike previous surveys of similar X-ray depth, such as the HELLAS2XMM (Baldi et al. 2002; Comastri et al. 2002; Brusa et al. 2003; Fiore et al. 2003; Mignoli et al. 2004; Perola et al. 2004), the XMDS is constructed to determine large scale structures and AGN correlation function.

An equatorial location (center of field RA = 02h 26m, dec = -4 deg) has been chosen to allow ground based coverage for follow-up observations from both emispheres. High galactic latitude and the absence of bright X-ray sources were also required. The region is covered by 19 *XMM - Newton* pointings, with a nominal exposure of 20 ksec each. U, B, V, R and I photometry have already been obtained in the VIMOS VLT Deep Survey (VVDS) context at a depth equivalent to $I_{AB} = 25.3$ over 1 deg^2 (Le Fèvre et al. 2004a;

McCracken et al. 2003; Radovich et al. 2004), a spectroscopic survey is in progress (Le Fèvre et al. 2004b) and a radio survey at 1.4 GHz has been completed at VLA (Bondi et al. 2003).

The XMDS pointings lie at the heart of the larger and shallower XMM Large Scale Structure (XMM – LSS) Survey (Pierre et al. 2001a,b), a large area survey whose objective is to study the large scale distribution and clustering properties of the matter traced by galaxy clusters. The coverage of the XMM – LSS (and XMDS) area by associated surveys in the radio, IR, optical and UV bands is in progress.

2. X-RAY DATA REDUCTION

We have analyzed the X-ray observations using a pipeline essentially identical to the one developed for the HELLAS2XMM survey (Baldi et al. 2002). We used the *XMM-Newton* Science Analysis System (XMM – SAS) v 5.4.1. The analysis is done on the merged event files from all the three imaging instruments (EPIC MOS1, EPIC MOS2 and EPIC pn) in several distinct X-ray bands: $0.3-0.5, 0.5-2, 2-4.5, 4.5-10$ and $2-10$ keV. We obtain count rates and fluxes for each energy band and hardness ratio between different bands, with their errors. Fluxes are computed for a power law spectrum with $\Gamma = 1.7$ and $N_H = 2.61 \times 10^{20}$ cm^{-2}. As a final step, only the sources which have a probability that counts originate from a background fluctuation $P < 2 \times 10^{-4}$ in at least one energy band have been considered for insertion in our database.

At the present time we have analyzed each pointing independently, despite the fact that the fields of view of adjacent *XMM* pointings overlap. The same object could therefore be detected more times, once in each fields.

We detected 1322 X-ray sources in the 18 useful fields that we have analyzed, including multiple detections in overlapping fields; the fraction of multiple detections is abount 15%. The flux range of the whole sample is about $10^{-16} - 10^{-12}$ erg cm^{-2} s^{-1} in the $0.5-2$ keV band.

All the X-ray related quantities are part of a database which also includes data from associated surveys in other wavebands and will hold the XMDS Master Catalogue. While such web site[1] is currently open for public browsing, access to the actual database tables is so far restricted to the members of the XMDS and XMM – LSS teams.

3. THE 4 σ SAMPLE

In order to obtain a statistically very reliable sample, we selected all X-ray detections above 4 σ level in at least one energy band, obtaining 536 independent X-ray sources (i.e. excluding multiple detections in adjacent pointings). A detailed analysis was performed in the area already covered by the VVDS photometry; the 4 σ VVDS sample consists of 286 independent X-ray sources. About 97% of them are detected in the $0.5-2$ keV band, while only $\sim 3\%$ are detected in the $2-10$ keV band only and none in the $4.5-10$ keV band only, suggesting that peculiar or highly absorbed spectra are not common in this sample. This is confirmed by the distribution of hardness ratios, as shown in section 4.

Their flux distribution is shown in Fig. 1 for $0.5-2$ keV (left panel) and $2-10$ keV (right panel) bands.

For optical identifications, we inspected I band images ($40'' \times 40''$ centered on the X-ray position) with a search radius of $6''$. We consider an X-ray source as identified if there is a single conterpart in the search radius or if there is an object brighter than at

[1] `http://cosmos.mi.iasf.cnr.it/~lssadmin/Website/LSS/`

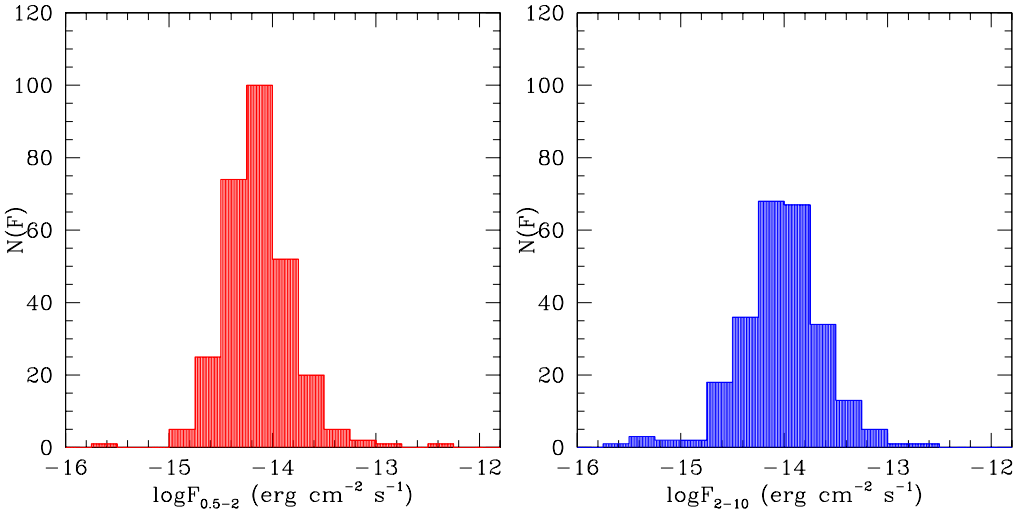

Fig. 1. Left panel: Flux distribution of the 4 σ VVDS sample in the $0.5-2$ keV band. Right panel: the same distribution in the $2-10$ keV band.

least 2 magnitudes with respect to the others within $6''$, or if there is within the search radius an optical object also associated with a radio source.

We used our "high confidence" identifications to correct the X-ray astrometry of the *XMM* pointings by means of SAS tasks. We found that the shift is small (usually 1 or $2''$); only one pointing was affected by a $\sim 4''$ shift. After astrometric correction, we obtained further identifications. We have at present 232 high confidence identifications (about 81% of the 4 σ VVDS sample). We also have 4 X-ray sources for which no optical counterparts at a depth equivalent to $I_{AB} = 25.3$ has been found within $6''$ (hereafter "blank fields") and 2 identifications with radio sources without optical counterparts. For the remaining 48 X-ray sources, the optical identification is ambiguous, because there are 2 or more optical objects with comparable magnitude in the search radius.

We *a posteriori* computed for each optical object within $6''$ the probability that it is a spurious association with the X-ray source:

$$P = 1 - exp(-d^2 \pi n(< m)) \quad (1)$$

where d is the offset between the X-ray and optical posistions and $n(< m)$ is the surface density of optical objects brighter than the magnitude m of the possible association. We chose $P = 0.01$ as a threshold to accept or reject an identification and found a good agreement with our visual identification criteria: only $\sim 11\%$ of our high confidence identifications have $P > 0.01$ and $\sim 58\%$ of them have $0.01 < P < 0.02$, while for most of residual X-ray sources all objects within the search radius have $P > 0.01$.

We show in Fig. 2 the R - magnitude distribution of our high confidence identifications (solid histogram) and for optical objects within $6''$ from the "ambiguously identified" sources (dashed histogram): the two distributions are quite different, with the former peaking at R $\sim$ 21 and the latter peaking at R $\sim$ 24; the optical spectroscopic follow-up for many of the ambiguously identified sources would therefore be difficult with the present facilities.

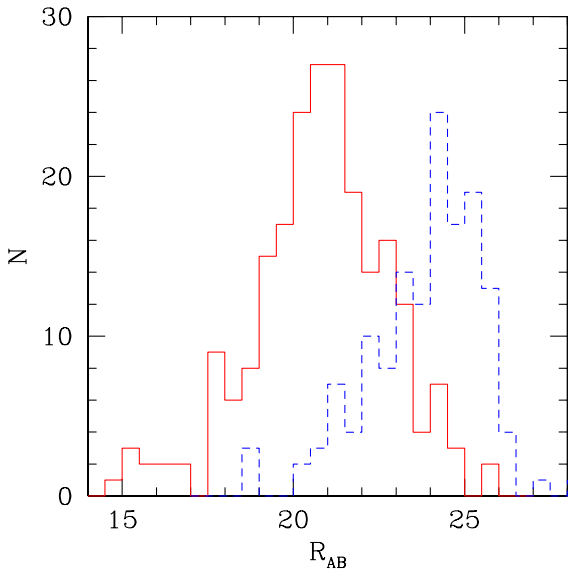

Fig. 2. R - magnitude distribution for identified sources (solid histogram) and for optical objects within 6″ from the "ambiguously identified" sources (dashed histogram) in the 4 σ VVDS sample.

4. DISCUSSION

We present in Fig. 3 the X-ray - to - optical ratio versus the X-ray flux ($2-10$ keV band) for identified sources ("blank fields" and radio identifications without optical counterparts are plotted as lower limits). 82% of them lie in the region of classical AGNs ($-1 < \log(\mathrm{F}_X/\mathrm{F}_R) < 1$), $\sim 9\%$ is in the starburst - normal galaxy range ($\log(\mathrm{F}_X/\mathrm{F}_R) < -1$), and about the same fraction (including "blank fields") is in the candidate obscured AGN region ($\log(\mathrm{F}_X/\mathrm{F}_R) > 1$). The percentage of high X/O sources is lower than in other X-ray surveys of similar depth (see e.g. Fiore et al. 2003); given that the sample is not fully identified and the high confidence identifications are by definition the optically brightest, the fraction of sources with $\log(\mathrm{F}_X/\mathrm{F}_R) > 1$ in the whole sample could be higher. On the other hand, we know that the number of hard sources in our sample is small (see previous section), so we do not expect to find many other sources with high X-ray - to - optical ratio.

The small number of peculiar sources is also confirmed by hardness ratio analysis. In Fig. 4 we plot the hardness ratio distribution of the 4 σ VVDS sample. Hardness ratio are defined as:

$$\mathrm{HR}_{cb} = \frac{CR_{2-4.5} - CR_{0.5-2}}{CR_{2-4.5} + CR_{0.5-2}} \tag{2}$$

$$\mathrm{HR}_{dc} = \frac{CR_{4.5-10} - CR_{2-4.5}}{CR_{4.5-10} + CR_{2-4.5}} \tag{3}$$

where CR are count rates in the various energy bands. Only 2% of sources have $\mathrm{HR}_{cb} > 0$ and none have both HR_{cb} and $\mathrm{HR}_{dc} > 0$.

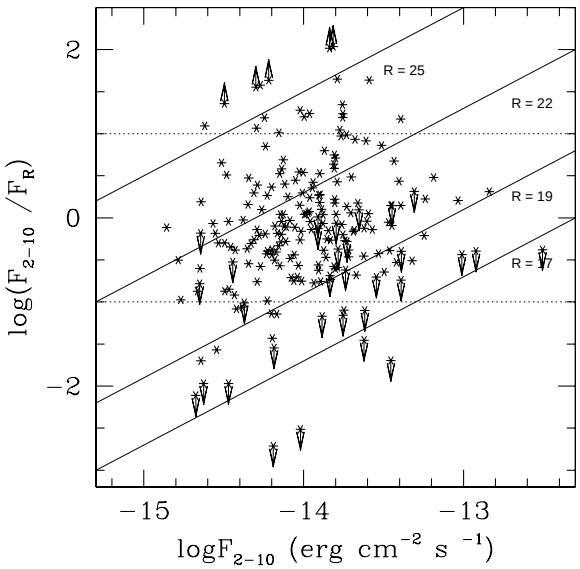

Fig. 3. X-ray (2 − 10 keV)/optical (R band) ratio vs X-ray flux for identified sources in the 4 σ VVDS sample. Upper limits are sources for which optical magnitudes are likely underestimated (saturated or border or masked sources), while lower limits are for "blank fields" and radio identifications without optical counterparts. Horizontal lines at ± 1 enclose the region of classical AGNs, starburst galaxies are at < -1, candidate obscured AGNs at > 1.

Also shown in Fig. 4 as dotted lines are the loci of stars and type I AGNs as defined by Della Ceca et al. (2004): most of stars should have $\mathrm{HR}_{cb} < -0.75$, while 90% of type I AGNs should lie in the range $-0.75 < \mathrm{HR}_{cb} < -0.35$. We have 8 reliable identifications with stars (objects also catalogued in SIMBAD and one with optical spectrum) and all but one have $\mathrm{HR}_{cb} > -0.75$. We must note that our hardness ratios are computed from the three cameras combined (see Baldi et al. 2002), while Della Ceca et al. (2004) use hardness ratios from the MOS2 alone, however comparisons we did between hardness ratios computed using single cameras and the three cameras combined show a good agreement.

As shown by Della Ceca et al. (2004), hardness ratio together with X-ray to - optical ratio allows to discriminate between stars and extragalactic sources: stars should be confined by $\mathrm{HR}_{cb} < -0.75$ and $\log(\mathrm{F}_X/\mathrm{F}_R) < -1$, while most of type I AGNs should lie at $-0.75 < \mathrm{HR}_{cb} < -0.35$ and $-0.5 < \log(\mathrm{F}_X/\mathrm{F}_R) < 1$. We present the same plot in Fig. 5: the box defined by dotted lines is the locus of stars, while the one defined by dashed lines is the locus of AGNs. Stars appear to be confined in the dotted box, and preliminary results from VVDS spectroscopy show that broad line QSOs seem to concentrate at $\log(\mathrm{F}_X/\mathrm{F}_R) \sim 0$ and $\mathrm{HR}_{cb} < -0.5$. We therefore confirm that this is a good criterium to separate stars from extragalactic sources.

5. CONCLUSIONS

We have analyzed 18 of the 19 *XMM* pointings of the XMDS, finding 1322 X-ray sources.

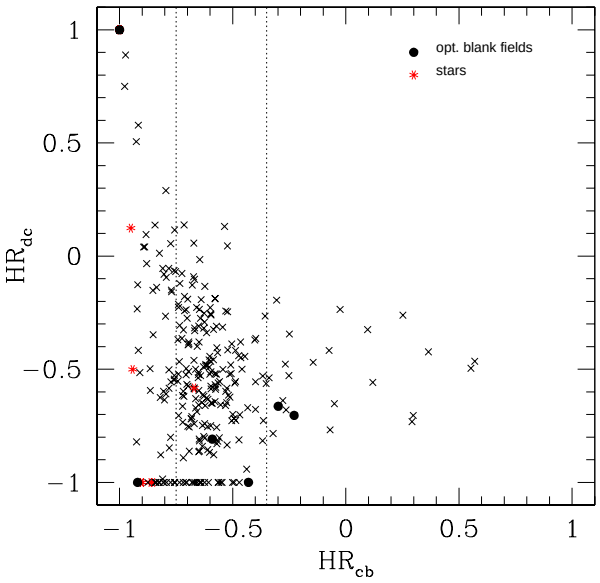

Fig. 4. Distribution of hardness ratios for the 4 σ VVDS sample. Energy bands are defined as: b: $0.5-2$, c: $2-4.5$, d: $4.5-10$ keV. Filled circles are blank fields. Dotted lines mark star and AGN regions: most of stars should have $\mathrm{HR}_{cb} < -0.75$, while most of type I AGNs should have $-0.75 < \mathrm{HR}_{cb} < -0.35$ (Della Ceca et al. 2004). Our identifications with stars are marked with red asterisks.

We then selected a restricted, statistically reliable sample (the 4 σ VVDS sample) of 286 X-ray sources, for which we have multiwavelength information: 81% of them have an optical high confidence identification.

Our sample is mainly soft: only 2% of sources are detected above 4 σ level in the $2-10$ keV band only. As a consequence, the number of peculiar sources is small and we have only $\sim 9\%$ of optically identified objects with X-ray - to - optical ratio in the range of candidate obscured AGNs. We note however that this value could be slightly higher because the 4 σ sample is not fully identified and reliable identifications are by definition the optically brightest objects.

We confirm that hardness ratios, joined with X-ray - to - optical ratio, is an useful tool to discriminate between stars and extragalactic population.

In the future we plan to continue the identification work and study in greater detail multiwavelength (X-ray, optical and radio) properties of the 4 σ VVDS sample. We are also checking the robustness of X-ray products (positions, fluxes and hardness ratios) before releasing the X-ray catalogue.

REFERENCES

Baldi, A. et al. 2002, ApJ 564, 190
Bondi, M. et al. 2003, A&A 403, 857
Brusa, M. et al. 2003, A&A 409, 65
Comastri, A. et al. 2002, ApJ 571, 771
Della Ceca, R. et al. 2004, A&A accepted, astro-ph/0407481

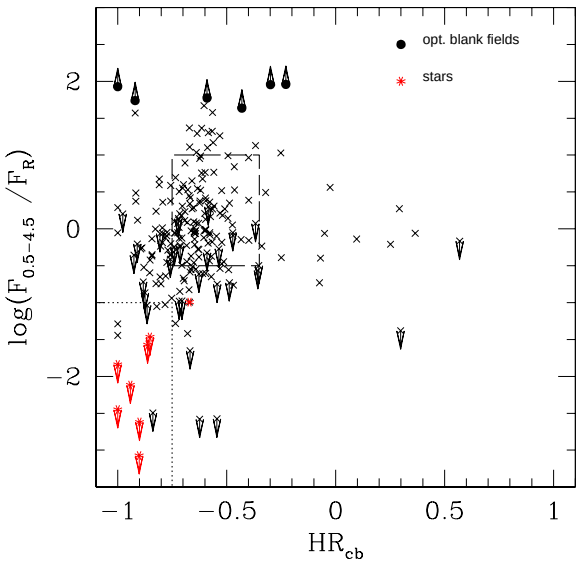

Fig. 5. X-ray $(0.5-4.5)$ /optical ratio vs hardness ratio for sources of the 4 σ VVDS sample. Simbols are as in Fig. 3 and Fig. 4. Dotted lines mark the locus of stars, while box defined by dashed lines is locus of type I AGNs.

Fiore, F. et al. 2003, A&A 409, 79
Le Fèvre, O. et al. 2004, A&A 417, 839
Le Fèvre, O. et al. 2004, in the Proceedings of the ESO/USM/MPE Workshop on "Multiwavelength Mapping of Galaxy Formation and Evolution", eds. R. Bender and A. Renzini, astro-ph/0402203
McCracken, H. J. et al. 2003, A&A 410, 17
Mignoli, M. et al. 2004, A&A 418, 827
Perola, G. C. et al. 2004, A&A 421, 491
Pierre, M. et al. 2001, ESO Messenger, 105, 32 (Pierre et al. 2001a)
Pierre, M, Valtchanov, I. & Refregier, in the Proceedings of the Conference "New Visions of the X-ray Universe in the XMM-Newton and Chandra Era" 26-30 November 2001, ESTEC, NL, astro-ph/0202117 (Pierre et al. 2001b)
Radovich, M. et al. 2004, A&A 417, 51